Nature of $\Lambda(1405)$

Masahiro Kimura,[1] Takahiko Miyakawa,[2] Akira Suzuki,[3] Miho Takayama,[4] K. Tanaka,[5] and Atsushi Hosaka[6]
[1]*Department of Electronics Engineering, Suwa College, Chino, Nagano, Japan*
[2]*Department of Physics, Tokyo Metropolitan University, Hachioji, Tokyo, Japan*
[3]*Department of Physics, Science University of Tokyo, Shinjuku, Tokyo, Japan*
[4]*Research Center for Nuclear Physics, Osaka University, Ibaraki, Osaka, Japan*
[5]*Department of Physics, University of Alberta, Edmonton, Alberta, Canada T6G 2J1*
[6]*Division of Liberal Arts, Numazu College of Technology, Numazu, Shizuoka, Japan*
(Received 7 September 1999; published 22 June 2000)

We study the structure of $\Lambda(1405)$ by means of a coupled-channel potential model and by fitting low-energy $\bar{K}N$ data, including the K^-p scattering length obtained from the latest x-ray measurements of the kaonic hydrogen atom. From the best fit obtained, we find two possible interpretations of $\Lambda(1405)$, either as (1) the 70^- three-quark state strongly coupled with $\bar{K}N$ and $\pi\Sigma$ or (2) a $\pi\Sigma$ resonance and/or an unstable $\bar{K}N$ bound state. In the latter case, the three-quark state that belongs to the 70^- multiplet is located slightly above the $\bar{K}N$ threshold and results in a sharp resonance peak in the K^-p elastic cross section at laboratory momentum 170 MeV/c. To explore these possibilities, measurements of the $\pi\Sigma$ invariant mass distribution and the K^-p cross sections with finer resolution are required.

PACS number(s): 36.10.Gv, 13.75.Jz, 14.20.Jn, 14.40.Aq

I. INTRODUCTION

The interpretation of $\Lambda(1405)$ — either as an elementary baryon with three-quark structure or a meson-baryon composite — has been controversial for the last few decades. It has been a key issue in theoretical studies of the $\bar{K}N$ system at low energies and particularly in attempts at resolving the so-called kaonic hydrogen puzzle [1–8]. The puzzle was concerned with an apparent discrepancy between the $1S$ level shift of the kaonic hydrogen atom determined from measurements of the atomic x rays [9–11] and that from the low-energy $\bar{K}N$ scattering data [1,5,12–14]. The atomic data indicated a downward shift of the $1S$ level, while the scattering data were extrapolated to the K^-p threshold to predict an upward shift [15]. The puzzle itself, however, has been resolved recently by new elaborate measurements of x rays from the atom, which revealed an upward shift of the $1S$ level [16]:

$$\epsilon + i\frac{\Gamma}{2} = -323 \pm 63 \pm 11 + \frac{i}{2}(407 \pm 208 \pm 100) \text{ eV}, \quad (1)$$

where the first and second errors correspond to the statistical and systematic errors, respectively. Through the formula of Deser *et al.* [17], the above shift and width of the $1S$ level can be converted to the K^-p scattering length as[1]

$$A_{K^-p} = (-0.78 \pm 0.18) + i\,(0.49 \pm 0.37) \text{ fm}, \quad (2)$$

where the errors have been estimated simply by adding those arising from the statistical and systematic errors in Eq. (1). This is compatible with the K^-p scattering length extracted from the scattering data. For example, using the $\bar{K}N$ scattering lengths in isospin channels $I=0$ and 1 of Ref. [12],

$$A_0 = -1.60 + i\,0.75 \text{ fm},$$

$$A_1 = 0.08 + i\,0.69 \text{ fm}, \quad (3)$$

and taking their average, we have $A_{K^-p} = -0.76 + i\,0.72$ fm.

The reason why the structure of $\Lambda(1405)$, observed as a resonance in the $\pi\Sigma$ invariant mass distribution, was a crucial point in explaining the puzzle is that $\Lambda(1405)$ lies just 25 MeV below the $\bar{K}N$ threshold and has a strong influence on the low-energy $\bar{K}N$ data. As one can see from Eq. (3), the negative $\mathrm{Re}\,A_{K^-p}$ is consistent with the negative $\mathrm{Re}\,A_0$. The negative $\mathrm{Re}\,A_0$ can be interpreted as due to the existence of an isosinglet bound state of $\bar{K}$ and N, and it may be understood by the picture that $\Lambda(1405)$ is (mostly) a $\bar{K}N$ and/or $\pi\Sigma$ composite [1,5,8,12–14]. However, this does not necessarily rule out the possibility that $\Lambda(1405)$ has an elementary-baryon component. The SU(3) quark model indeed predicts a three-quark state that has the same quantum numbers as $\Lambda(1405)$, as a member of the 70^- multiplet with two partners $\Lambda(1670)$ and $\Lambda(1800)$ of $J^\pi = 1/2^-$. In Ref. [3] it has been proposed that $\Lambda(1405)$ is dominantly this 70^- state and that its strong coupling with $\bar{K}N$ and $\pi\Sigma$ makes its mass much smaller than the other two members.

In this work, we address the question as to whether $\Lambda(1405)$ can be interpreted as the 70^- three-quark state, and if not, where the mass of the ''missing'' 70^- state can be. We study the coupled system of $\bar{K}N$ and $\pi\Sigma$ near the $\bar{K}N$ threshold by means of a coupled-channel potential model. To capture the essential features of the system in the energy

[1]The uncertainty in the formula of Deser *et al.* due to the extrapolation of the scattering amplitude from the K^-p threshold to the Coulomb level can be estimated [17], in this case, to be less than 2% ($\simeq 0.01$ fm) for both real and imaginary parts.

range considered, we mostly focus on the isosinglet states. We introduce an elementary particle with $J^\pi = 1/2^-$ which represents the 70^- three-quark state (we call it Λ_0) and assume that its bare mass lies within the low-energy region for $\bar{K}N$. We adopt a separable potential to describe the meson-baryon interaction and a Yukawa-type form for the Λ_0-meson-baryon coupling. For the isotriplet states, we simplify the problem by explicitly using the $\bar{K}N$ channel only and including the $\pi\Sigma$ and $\pi\Lambda$ channels by means of complex coupling constants. By fitting the low-energy $\bar{K}N$ data including the $K^- p$ scattering length in Eq. (2) and solving the eigenvalue problem for the isosinglet states, we examine the probabilities of the three-quark and meson-baryon components in $\Lambda(1405)$. Throughout this work, we assume isospin symmetry and neglect the mass differences among the particle channels of $\bar{K}N$ and those of $\pi\Sigma$.

In the next section, we solve the eigenvalue equation for the isosinglet states in the coupled-channel system, and in Sec. III we give formulations for the $\bar{K}N$ scattering states. Our main results are presented and discussed in Sec. IV.

II. EIGENVALUES IN ISOSINGLET STATES

We first consider the isosinglet states. We label the channels of Λ_0, $\pi\Sigma$, and $\bar{K}N$ as 0, 1, and 2, respectively. Accordingly we write the free Hamiltonians for these channels as H_0, H_1, and H_2. Then the total Hamiltonian is given by

$$H = H_0 + \sum_{i=1,2} H_i + \sum_{i=1,2} (V_{0i} + V_{i0}) + \sum_{i,j=1,2} V_{ij}^{(0)}, \quad (4)$$

where we have singled out the interaction terms involving channel 0. The subscripts in Eq. (4) represent the particle channels on which the operators act, and the superscript for the potential between two meson-baryon channels stands for isospin $I=0$. The particle channel (and isospin) subscripts of an operator indicate that the projection operators onto the corresponding spaces are attached to the operator. The operator $V_{ij}^{(0)}$, for example, acts on channel j and changes it to channel i in an isosinglet state.

We solve the eigenvalue equation

$$H|\Psi_\beta\rangle = E_\beta |\Psi_\beta\rangle, \quad (5)$$

where E_β is the eigenvalue for state β. When the real part of an eigenvalue is located below the $\bar{K}N$ threshold but above the $\pi\Sigma$ threshold, the eigenvalue becomes complex. When it appears on the second Riemann sheet of the complex energy plane, we call it a $\pi\Sigma$ resonance and/or an unstable $\bar{K}N$ bound state. We expand $|\Psi_\beta\rangle$ in terms of complete sets spanning the three channel spaces. They are defined by

$$H_0|\Lambda_0\rangle = M_0|\Lambda_0\rangle, \quad (6)$$

$$(H_i + V_{ii}^{(0)})|\phi_{i,\mu}\rangle = E_{i,\mu}|\phi_{i,\mu}\rangle, \quad i=1,2, \quad (7)$$

in center-of-mass coordinates, where M_0 is the bare mass of Λ_0 and taken to be a free parameter. In Eq. (7), μ denotes an eigenstate in channel i. We assume that the $\pi\Sigma$ channel has no bound state and thus the scattering states form a complete set in this channel. On the other hand, there may be a bound state(s) in the $\bar{K}N$ channel, so, in general, μ for channel 2 in Eq. (7) represents a bound state or a scattering state. We expand $|\Psi_\beta\rangle$ using these complete sets:

$$|\Psi_\beta\rangle = \alpha_0|\Lambda_0\rangle + \sum_{i=1,2}\sum_{\mu} \alpha_{i,\mu}|\phi_{i,\mu}\rangle, \quad (8)$$

where α_0 and $\alpha_{i,\mu}$ are the probability amplitudes for the states $|\Lambda_0\rangle$ and $|\phi_{i,\mu}\rangle$ contained in $|\Psi_\beta\rangle$, respectively. Therefore

$$P(\Lambda_0) = |\alpha_0|^2, \quad (9)$$

$$P(\pi\Sigma) = \sum_k |\alpha_{1,k}|^2, \quad (10)$$

$$P([\bar{K}N]_B) = |\alpha_{2,b}|^2, \quad (11)$$

$$P([\bar{K}N]_S) = \sum_k |\alpha_{2,k}|^2 \quad (12)$$

are the probabilities with which one finds the three-quark state, the $\pi\Sigma$ scattering states, a $\bar{K}N$ bound state, and the $\bar{K}N$ scattering states in $|\Psi_\beta\rangle$, respectively.

For the Λ_0-meson-baryon interaction in Eq. (4) we adopt a Yukawa-type form

$$\langle\Lambda_0|V_{0i}|\phi_{i,\mu}\rangle = \lambda_i\langle v_i|\phi_{i,\mu}\rangle, \quad i=1,2. \quad (13)$$

For the meson-baryon potential $V_{ij}^{(0)}$ we assume the following separable form:

$$\langle\phi_{i,\nu}|V_{ij}^{(0)}|\phi_{j,\mu}\rangle = \eta_{ij}^{(0)}\langle\phi_{i,\nu}|v_i\rangle\langle v_j|\phi_{j,\mu}\rangle, \quad i,j=1,2, \quad (14)$$

where λ_i and $\eta_{ij}^{(0)}$ are real coupling constants.

We first solve Eq. (7) for channels 1 and 2 with the potential given by Eq. (14). For the scattering states we have

$$\langle v_i|\phi_{i,k}\rangle = \frac{v_{i,k}}{1 - \eta_{ii}^{(0)} I_i(E_{i,k})}, \quad (15)$$

where

$$I_i(E) = \langle v_i|g_i(E)|v_i\rangle, \quad (16)$$

$$g_i(E) = (E - H_i + i\epsilon)^{-1}, \quad (17)$$

and

$$v_{i,k} = \langle \boldsymbol{k}|v_i\rangle. \quad (18)$$

Here $|\boldsymbol{k}\rangle$ is a plane wave state in the center-of-mass system of channel i with momentum $\boldsymbol{k}$, whose magnitude is determined by the channel energy $E_{i,k}$ through the relation

$$E_{i,k} = \omega_{i,k} + \epsilon_{i,k}, \quad (19)$$

with $\omega_{i,k}=\sqrt{m_i^2+k^2}$ and $\epsilon_{i,k}=\sqrt{M_i^2+k^2}$. The m_i and M_i are the meson and baryon masses in channel i:

$$m_i=\begin{cases} m_\pi=135 \text{ MeV}, \\ m_K=494 \text{ MeV}, \end{cases}$$

$$M_i=\begin{cases} M_\Sigma=1192 \text{ MeV} & \text{for } i=1, \\ M_N=938 \text{ MeV} & \text{for } i=2. \end{cases} \tag{20}$$

If there is a solution for

$$1-\eta_{22}^{(0)}I_2(E_{2,b})=0, \tag{21}$$

it is a bound state with eigenvalue $E_{2,b}$ in the $\bar{K}N$ channel. The normalized wave function for this bound state is given by

$$|\phi_{2,b}\rangle=Z_2(E_{2,b})^{-1/2}g_2(E_{2,b})|v_2\rangle, \tag{22}$$

where

$$Z_i(E)=\langle v_i|g_i(E)^\dagger g_i(E)|v_i\rangle. \tag{23}$$

Note that $|\phi_{2,b}\rangle$ is the only bound state for the potential given by Eq. (14) and $E_{2,b}$ is real.

Using these eigenstates of Eq. (7), we can now solve Eq. (5). With the help of the equality

$$\langle v_i|(E-H_i-V_{ii}^{(0)}+i\epsilon)^{-1}|v_i\rangle=\frac{I_i(E)}{1-\eta_{ii}^{(0)}I_i(E)}, \tag{24}$$

we can express $\alpha_{i,\mu}$ in Eqs. (10)–(12) in terms of α_0 as

$$\alpha_{1,\mu}=\frac{\lambda_1\{1-\eta_{22}^{(0)}I_2(E_\beta)\}+\lambda_2\eta_{12}^{(0)}I_2(E_\beta)}{d^{(0)}(E_\beta)} \times\langle\phi_{1,\mu}|g_1(E_\beta)|v_1\rangle\alpha_0, \tag{25}$$

$$\alpha_{2,\mu}=\frac{\lambda_2\{1-\eta_{11}^{(0)}I_1(E_\beta)\}+\lambda_1\eta_{21}^{(0)}I_1(E_\beta)}{d^{(0)}(E_\beta)} \times\langle\phi_{2,\mu}|g_2(E_\beta)|v_2\rangle\alpha_0, \tag{26}$$

where

$$d^{(0)}(E)=[1-\eta_{11}^{(0)}I_1(E)][1-\eta_{22}^{(0)}I_2(E)] -\eta_{12}^{(0)}\eta_{21}^{(0)}I_1(E)I_2(E). \tag{27}$$

The eigenvalues $\{E_\beta\}$ of our coupled-channel system are obtained as complex roots of

$$\begin{vmatrix} 1-\tilde{\eta}_{11}^{(0)}(E_\beta)I_1(E_\beta) & -\tilde{\eta}_{12}^{(0)}(E_\beta)I_1(E_\beta) \\ -\tilde{\eta}_{21}^{(0)}(E_\beta)I_2(E_\beta) & 1-\tilde{\eta}_{22}^{(0)}(E_\beta)I_2(E_\beta) \end{vmatrix}=0, \tag{28}$$

where

$$\tilde{\eta}_{ij}^{(0)}(E)=\eta_{ij}^{(0)}+\frac{\lambda_i\lambda_j}{E-M_0}. \tag{29}$$

When we solve Eq. (28), the complex function $I_i(E_\beta)$ must be analytically continued to the appropriate Riemann sheet in the complex energy plane. The normalization condition for $|\Psi_\beta\rangle$ requires

$$|\alpha_0|=\left[1+\left|\frac{\lambda_1\{1-\eta_{22}^{(0)}I_2(E_\beta)\}+\lambda_2\eta_{12}^{(0)}I_2(E_\beta)}{d^{(0)}(E_\beta)}\right|^2 Z_1(E_\beta) +\left|\frac{\lambda_2\{1-\eta_{11}^{(0)}I_1(E_\beta)\}+\lambda_1\eta_{21}^{(0)}I_1(E_\beta)}{d^{(0)}(E_\beta)}\right|^2 Z_2(E_\beta)\right]^{-1/2}, \tag{30}$$

where

$$Z_i(E_\beta)=-\frac{\mathrm{Im}[I_i(E_\beta)]}{\mathrm{Im}[E_\beta]}. \tag{31}$$

Now we can calculate all the probabilities defined by Eqs. (9)–(12) in the state $|\Psi_\beta\rangle$.

III. $\bar{K}N$ SCATTERING STATES

We fix the parameters by fitting the low-energy K^-p cross sections for elastic and inelastic processes, the K^-p scattering length, and the $\pi\Sigma$ invariant mass distribution below the $\bar{K}N$ threshold. In order to calculate these quantities, we need the $\bar{K}N$ scattering matrices in the isosinglet and isotriplet states.

For the isosinglet states, we denote the scattering matrix element from channel i to j by $T_{ij}^{(0)}(E)$ and define

$$\boldsymbol{T}^{(0)}(E)=\begin{pmatrix} T_{11}^{(0)}(E) & T_{12}^{(0)}(E) \\ T_{21}^{(0)}(E) & T_{22}^{(0)}(E) \end{pmatrix}. \tag{32}$$

When we eliminate the Λ_0 channel, the scattering matrices satisfy

$$\boldsymbol{T}^{(0)}(E)=\boldsymbol{V}^{(0)}(E)+\boldsymbol{V}^{(0)}(E)\boldsymbol{g}(E)\boldsymbol{T}^{(0)}(E), \tag{33}$$

where

$$\boldsymbol{V}^{(0)}(E)=\begin{pmatrix} |v_1\rangle\tilde{\eta}_{11}^{(0)}(E)\langle v_1| & |v_1\rangle\tilde{\eta}_{12}^{(0)}(E)\langle v_2| \\ |v_2\rangle\tilde{\eta}_{21}^{(0)}(E)\langle v_1| & |v_2\rangle\tilde{\eta}_{22}^{(0)}(E)\langle v_2| \end{pmatrix}, \tag{34}$$

$$\boldsymbol{g}(E)=\begin{pmatrix} g_1(E) & 0 \\ 0 & g_2(E) \end{pmatrix}. \tag{35}$$

We can solve Eq. (33) to obtain

$$\boldsymbol{T}^{(0)}(E)=\frac{\boldsymbol{N}^{(0)}(E)}{D^{(0)}(E)}, \tag{36}$$

where

$$\boldsymbol{N}^{(0)}(E)=\boldsymbol{V}^{(0)}(E)-[\,\tilde{\eta}_{11}^{(0)}(E)\,\tilde{\eta}_{22}^{(0)}(E)-\tilde{\eta}_{12}^{(0)}(E)\,\tilde{\eta}_{21}^{(0)}(E)] \times\begin{pmatrix} |v_1\rangle I_2(E)\langle v_1| & 0 \\ 0 & |v_2\rangle I_1(E)\langle v_2| \end{pmatrix} \tag{37}$$

and

$$D^{(0)}(E)=[1-\tilde{\eta}_{11}^{(0)}(E)I_1(E)][1-\tilde{\eta}_{22}^{(0)}(E)I_2(E)] -\tilde{\eta}_{12}^{(0)}(E)\,\tilde{\eta}_{21}^{(0)}(E)I_1(E)I_2(E). \tag{38}$$

Note that the zeros of $D^{(0)}(E)$ on the complex energy plane are the eigenvalues $\{E_\beta\}$ that are the roots of Eq. (28).

As for the isotriplet state, we explicitly consider the $\bar{K}N$ channel only and take into account the $\pi\Sigma$ and $\pi\Lambda$ channels by a complex coupling constant. We assume a separable form for the $\bar{K}N$ potential,

$$V_{22}^{(1)}=|v_2\rangle\,\eta_{22}^{(1)}\langle v_2|, \tag{39}$$

where $\eta_{22}^{(1)}$ is complex. Thus the $\bar{K}N$ scattering matrix in the isotriplet state is given by

$$T_{22}^{(1)}(E)=\frac{|v_2\rangle\,\eta_{22}^{(1)}\langle v_2|}{1-\eta_{22}^{(1)}I_2(E)}. \tag{40}$$

We calculate the scattering matrices

$$T_{K^-p\to K^-p}(E)=\frac{1}{2}[T_{22}^{(1)}(E)+T_{22}^{(0)}(E)], \tag{41}$$

$$T_{K^-p\to \bar{K}^0n}(E)=\frac{1}{2}[T_{22}^{(1)}(E)-T_{22}^{(0)}(E)], \tag{42}$$

$$T_{K^-p\to \pi^0\Sigma^0}(E)=-\frac{1}{\sqrt{6}}T_{21}^{(0)}(E). \tag{43}$$

The cross sections are given by

$$\sigma_{a\to b}(E)=4\pi\frac{q}{k}\left|-\frac{\sqrt{\omega_k\omega_q\epsilon_k\epsilon_q}}{2\pi E}T_{a\to b}(E)\right|^2, \tag{44}$$

where the subscripts a and b represent the initial and final particle channels, respectively, and k and q are magnitudes of their center-of-mass momenta. We have ignored the threshold difference between the K^-p and $\bar{K}^0n$ channels.

In addition to the scattering cross sections given above, we calculate the invariant mass distribution of the isosinglet $\pi\Sigma$ channel, $W_{\pi\Sigma}(E)$. Apart from a constant factor, it is given by

$$W_{\pi\Sigma}(E)\propto k\,|T_{11}^{(0)}(E)|^2, \tag{45}$$

where k is the momentum in the $\pi\Sigma$ channel. In the vicinity of the $\Lambda(1405)$ resonance we write $T_{11}^{(0)}$ as

$$T_{11}^{(0)}(E)=\frac{1}{\rho_1(E)}\frac{\Gamma/2}{E-E_R+i\Gamma/2}, \tag{46}$$

TABLE I. The low-energy K^-p cross sections for elastic and inelastic processes.

k (MeV/c)	$\sigma_{K^-p\to K^-p}$ (mb)	$\sigma_{K^-p\to \bar{K}^0n}$ (mb)	$\sigma_{K^-p\to \pi^0\Sigma^0}$ (mb)
110	87.29± 10.71	29.2± 6.3	
120			19.9± 8.6
130	79.22± 6.28		
140		33.4± 5.6	
150	69.61± 5.39		
160		17.6± 2.4	16.1± 6.9
170	75.76± 4.24		
180		17.9± 2.1	
190	59.09± 3.41		
200		15.8± 1.7	10.5± 4.0

where $\rho_1(E)$ is the density of states for the $\pi\Sigma$ channel, and E_R and Γ are obtained from

$$\mathrm{Re}[D^{(0)}(E_R)]=0 \tag{47}$$

and

$$\Gamma=\frac{2\,\mathrm{Im}[\,D^{(0)}(E_R)\,]}{\{d\,\mathrm{Re}[\,D^{(0)}(E)\,]/dE\}_{E=E_R}}. \tag{48}$$

Note that in general the pole of $T_{11}^{(0)}(E)$ does not coincide with any of the (complex) eigenvalues E_β.

We choose a Gaussian function for the form factor of the separable potentials:

$$v_{i,k}=\frac{\exp[-k^2/\Lambda^2]}{\sqrt{2\omega_{i,k}}}, \tag{49}$$

where Λ is the cutoff momentum. The parameters which we have to determine are λ_1, λ_2, $\eta_{11}^{(0)}$, $\eta_{22}^{(0)}$, $\eta_{12}^{(0)}=\eta_{21}^{(0)}$, $\eta_{22}^{(1)}$, M_0, and Λ. In order to reduce the number of parameters, we utilize the relation

$$\lambda_1=\frac{3}{2}\lambda_2, \tag{50}$$

which emerges from the SU(3) quark model, and fix Λ to be[2]

$$\Lambda=2000\ \ \mathrm{MeV}. \tag{51}$$

Thus there are six parameters left.

The experimental data which we use to fix the parameters are the low-energy K^-p cross sections for elastic and inelastic processes listed in Table I [18], the K^-p scattering length given in Eq. (2), and the $\Lambda(1405)$ resonance [19] with

$$(E_R,\ \Gamma/2)=(1406.5\pm 4.0, 25\pm 1)\ \ \mathrm{MeV}. \tag{52}$$

[2]We also performed calculations with $\Lambda=1000$ MeV and found that the results are not changed by the magnitude of the cutoff momentum.

TABLE II. Parameters which fit the experimental data. The last column gives the binding energy of the isosinglet $\bar{K}N$ bound state emerging from the potential $V_{22}^{(0)}$ when no coupling with the other channels is assumed.

	$\eta_{11}^{(0)}$	$\eta_{22}^{(0)}$	$\eta_{12}^{(0)}$	$\eta_{22}^{(1)}$	λ_2	M_0 (MeV)	$E_{2,b}$ (MeV)
Set A	−4.2273	−6.9098	1.3259	−4.4193-*i*4.8107	0.1141	1429.8	1426.8
Set B	−3.6145	−6.7145	−1.6698	−4.2195-*i*2.8561	0.0190	1449.7	1429.4

IV. RESULTS AND DISCUSSIONS

We have found two sets of parameters which yield the best fit of the experimental data. We call them set A and set B. These parameters are listed in Table II, along with the binding energy of the isosinglet KN bound state emerging from Eq. (21) when the given set of parameters is used. Once the parameters are obtained, we can evaluate the eigenvalues $\{E_\beta\}$ by solving Eq. (28) numerically and calculate the probabilities defined by Eqs. (9)–(12).

In set A the mass of Λ_0 is located at

$$M_0 = 1429.8 \ \text{MeV}, \tag{53}$$

which is approximately 2 MeV below the $\bar{K}N$ threshold. Figure 1 shows the $K^- p$ elastic cross section calculated from set A. Using the parameters of set A, we have found two roots for Eq. (28) whose real parts are located below the KN threshold and above the $\pi\Sigma$ threshold. They appear on the second Riemann sheet of the complex energy plane. Therefore these roots can be interpreted as resonances in the $\pi\Sigma$ channel and/or unstable bound states in the $\bar{K}N$ channel.

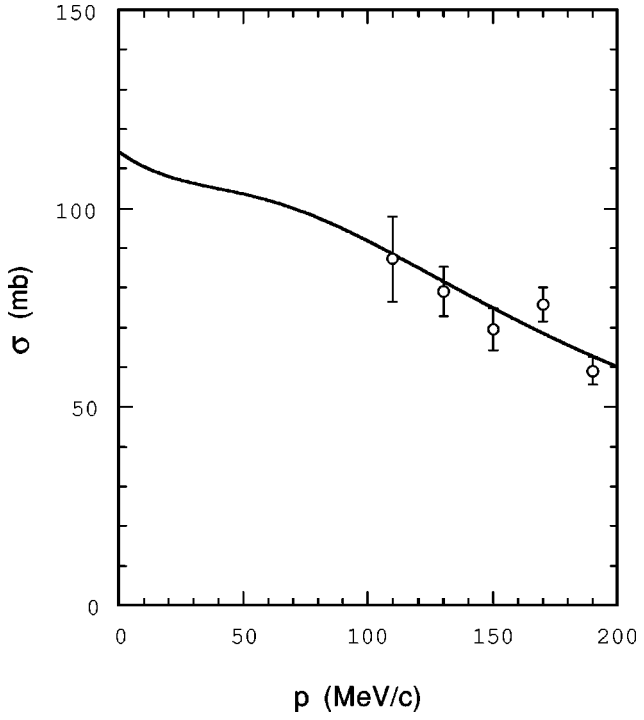

FIG. 1. The $K^- p$ elastic cross sections calculated with the parameters of set A.

These eigenstates show up as two peaks in the $\pi\Sigma$ invariant mass distribution. The energy and width of the first one is

$$(E_R, \ \Gamma/2) = (1407.56, \ 25.12) \ \text{MeV}, \tag{54}$$

and we identify this state as $\Lambda(1405)$. The second one has a little higher energy and much smaller width: in fact, it is located too close to the $\Lambda(1405)$ peak and its width is too narrow to be resolved in the currently available data for the mass distribution. In Table III the probabilities to find Λ_0, the $\pi\Sigma$ scattering states, the KN bound state, and the KN scattering states in these eigenstates are given in percent. In both states the probability for Λ_0 is comparable with those for the $\pi\Sigma$ scattering states and the KN bound state. Therefore the $\Lambda(1405)$ resonance can be understood as arising from the three-quark state Λ_0 which strongly couples to the $\pi\Sigma$ and $\bar{K}N$ channels.

The key difference between set A and set B is that in set B, the mass of Λ_0 is above the $\bar{K}N$ threshold:

$$M_0 = 1449.7 \ \text{MeV}. \tag{55}$$

Again we found two roots for Eq. (28). One of them has its real part below the KN threshold, appearing on the second Riemann sheet of the complex energy plane. This state results in the $\pi\Sigma$ mass distribution as the $\Lambda(1405)$ peak, with

$$(E_R, \ \Gamma/2) = (1407.50, \ 25.13) \ \text{MeV}. \tag{56}$$

As can be see in Table III (the first line for set B), this state barely contains the three-quark state and it is composed dominantly of the $\pi\Sigma$ scattering states and the KN bound state. The other root was found on the third Riemann sheet of the complex energy plane, with its real part lying above the $\bar{K}N$ threshold. From the probabilities shown in Table III, this state can be interpreted as the three-quark state which is strongly coupled to the KN scattering states. This state has a

TABLE III. Eigenvalues E_β obtained from Eq. (28) and probabilities to find the three-quark state $[P(\Lambda_0)]$, the $\pi\Sigma$ scattering states $[P(\pi\Sigma)]$, the $\bar{K}N$ bound state $(P([\bar{K}N]_B))$, and the $\bar{K}N$ scattering states $(P([\bar{K}N]_S))$ in the corresponding eigenstates.

	E_β (MeV)	$P(\Lambda_0)$	$P(\pi\Sigma)$	$P([\bar{K}N]_B)$	$P([\bar{K}N]_S)$
	1424.71-*i*3.67	32.11	51.81	15.66	0.42
Set A	1427.68-*i*12.29	14.14	49.03	31.24	5.59
	1421.47-*i*19.92	0.25	48.33	35.05	16.37
Set B	1449.77-*i*0.05	44.51	0.70	0.05	54.74

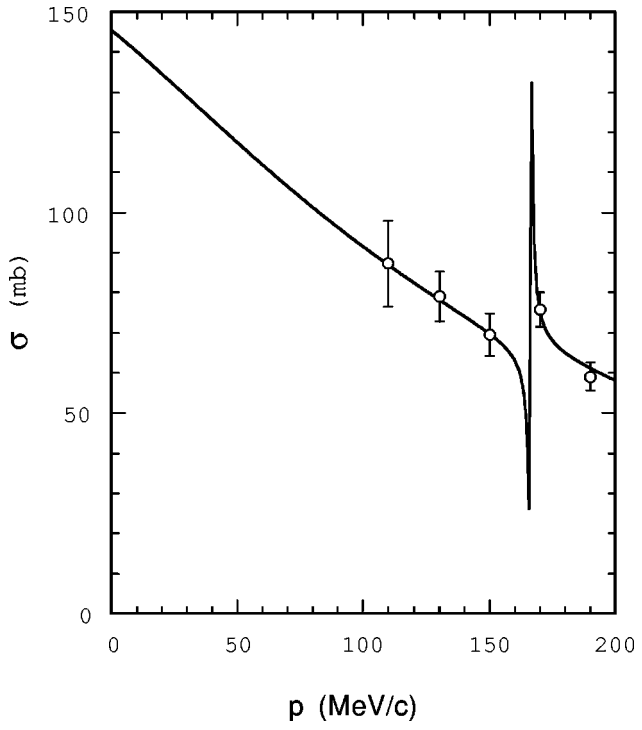

FIG. 2. The K^-p elastic cross sections calculated with the parameters of set B.

very narrow width and shows up in the K^-p elastic cross section as a small and sharp peak, as seen in Fig. 2. Very interestingly, this peak successfully reproduces the particular data point at laboratory momentum $k=170$ MeV/c. On the other hand, in Fig. 1 this point seems a little off the smooth curve of the cross section obtained from set A.

We should note here that the above values of M_0 are subject to uncertainty due to the mass difference between the particle channels of KN (or $\pi\Sigma$) which we have neglected in our calculations. In particular, in set A the difference between M_0 and the KN threshold is roughly the same as the mass difference between K^-p and $\bar{K}^0N$, and we cannot say for certain if M_0 is below or above the K^-p threshold. Furthermore, while the K^-p scattering length, Eq. (2), has been included at the KN threshold, the K^-p branching ratio data will put further constraints [20] on the KN amplitude at the threshold. If these data are included, M_0 in fits that correspond to the above two sets — especially set A — may be different from M_0 given in Eqs. (53) and (55). We have found, however, that for both sets A and B, the composition of $\Lambda(1405)$ as described above is not changed when M_0 is varied within a range of about 2 MeV.

In summary, we have studied whether or not $\Lambda(1405)$ can be interpreted as the three-quark state that belongs to the 70^- multiplet of the SU(3) quark model. We have used a simplified coupled-channel potential model and fit the low-energy KN scattering data, the K^-p scattering length determined from the latest measurements of atomic x rays, and the $\pi\Sigma$ mass distribution. Two sets of parameters which best fit these data have been found, with the bare mass of the three-quark state lying within the low-energy region around the KN threshold. The first set allows us to interpret $\Lambda(1405)$ as the three-quark state strongly coupled with the $\pi\Sigma$ and KN channels, as proposed in Ref. [3]. The second set, on the contrary, reproduces $\Lambda(1405)$ as a $\pi\Sigma$ resonance and/or an unstable KN bound state. For this set of parameters, the three-quark state manifests itself as a narrow resonance in the scattering region of KN and as a sharp peak in the K^-p elastic cross section around the data point at $k=170$ MeV/c.

We have thus two possibilities, if the bare mass of the 70^- three-quark state lies in the low-energy region for KN: the three-quark state gives rise to either $\Lambda(1405)$ or a sharp resonance in the KN scattering states — in the latter case $\Lambda(1405)$ is a meson-baryon composite. To explore these possibilities, measurements of the $\pi\Sigma$ mass distribution and the K^-p cross sections with finer resolution are required.

ACKNOWLEDGMENT

We would like to thank Yuki Nogami for many helpful comments and discussions.

[1] E. A. Veit, B. K. Jennings, A. W. Thomas, and R. C. Barrett, Phys. Rev. D **31**, 1033 (1985).
[2] B. K. Jennings, Phys. Lett. B **176**, 229 (1986).
[3] M. Arima and K. Yazaki, Nucl. Phys. **A506**, 553 (1990); M. Arima, S. Matsui, and K. Shimizu, Phys. Rev. C **49**, 2831 (1994).
[4] G. He and R. H. Landau, Phys. Rev. C **48**, 3047 (1993).
[5] P. B. Siegel and B. Saghai, Phys. Rev. C **52**, 392 (1995), see also earlier references therein.
[6] K. S. Kumar and Y. Nogami, Phys. Rev. D **21**, 1834 (1980).
[7] J. Schnick and R. H. Landau, Phys. Rev. Lett. **58**, 1719 (1987); P. J. Fink, Jr., G. He, R. H. Landau, and J. W. Schnick, Phys. Rev. C **41**, 2720 (1990).
[8] K. Tanaka and A. Suzuki, Phys. Rev. C **45**, 2068 (1992).
[9] J. D. Davies *et al.*, Phys. Lett. **83B**, 55 (1979).
[10] M. Izycki *et al.*, Z. Phys. A **297**, 11 (1980).
[11] P. M. Bird *et al.*, Nucl. Phys. **A404**, 482 (1983).
[12] Y.-A. Chao, R. W. Kraemer, D. W. Thomas, and B. R. Martin, Nucl. Phys. **B56**, 46 (1973).
[13] A. D. Martin, Phys. Lett. **65B**, 346 (1976); Nucl. Phys. **B179**, 33 (1981).
[14] R. H. Dalitz and J. G. McGinley, *Proceedings of the International Conference on Hypernuclear and Kaon Physics* (North-Holland, Heidelberg, 1982).
[15] In Ref. [8] within a coupled-channel potential scheme, a good overall fit to all the low-energy KN data that was consistent with the atomic data of Refs. [9–11] was obtained. However, the resulting K^-p scattering amplitude was quite different at low energies from the one determined earlier from the Coulomb-nuclear interference.

[16] M. Iwasaki *et al.*, Phys. Rev. Lett. **78**, 3067 (1997); T. M. Ito *et al.*, Phys. Rev. C **58**, 2366 (1998).
[17] S. Deser, M. L. Goldberger, K. Bauman, and W. Thirring, Phys. Rev. **96**, 774 (1954); T. H. Trueman, Nucl. Phys. **26**, 57 (1961).
[18] M. Sakitt *et al.*, Phys. Rev. **139**, B719 (1965); D. Evans *et al.*, J. Phys. G **9**, 885 (1983); J. K. Kim, Columbia University Report No. Nevis 149, 1966.
[19] C. Caso *et al.*, Eur. Phys. J. C **3**, 1 (1998).
[20] P. B. Siegel and W. Weise, Phys. Rev. C **38**, 2221 (1988).